Accepted Manuscript

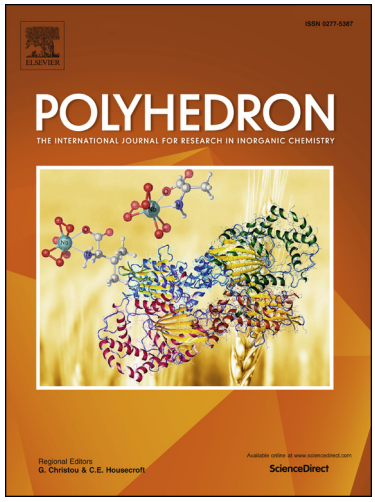

An unusual iminoacylation of 2-amino pyridyl thiazole: Synthesis, X-ray crystallography and DFT study of copper(II) amidine complexes and their cytotoxicity, DNA binding and cleavage study

Pradip Bera, Paula Brandão, Gopinath Mondal, Ananyakumari Santra, Abhimanyu Jana, Raveendra Babu Mokhamatam, Sunil Kumar Manna, Tarun Kanti Mandal, Pulakesh Bera

PII: S0277-5387(18)30799-X
DOI: https://doi.org/10.1016/j.poly.2018.11.069
Reference: POLY 13621

To appear in: *Polyhedron*

Received Date: 4 September 2018
Revised Date: 24 November 2018
Accepted Date: 28 November 2018

Please cite this article as: P. Bera, P. Brandão, G. Mondal, A. Santra, A. Jana, R.B. Mokhamatam, S.K. Manna, T.K. Mandal, P. Bera, An unusual iminoacylation of 2-amino pyridyl thiazole: Synthesis, X-ray crystallography and DFT study of copper(II) amidine complexes and their cytotoxicity, DNA binding and cleavage study, *Polyhedron* (2018), doi: https://doi.org/10.1016/j.poly.2018.11.069

This is a PDF file of an unedited manuscript that has been accepted for publication. As a service to our customers we are providing this early version of the manuscript. The manuscript will undergo copyediting, typesetting, and review of the resulting proof before it is published in its final form. Please note that during the production process errors may be discovered which could affect the content, and all legal disclaimers that apply to the journal pertain.

ACCEPTED MANUSCRIPT

An unusual iminoacylation of 2-amino pyridyl thiazole: Synthesis, X-ray crystallography and DFT study of copper(II) amidine complexes and their cytotoxicity, DNA binding and cleavage study

PradipBera,[a†] Paula Brandão,[b] Gopinath Mondal,[a] Ananyakumari Santra,[a] Abhimanyu Jana,[a] Raveendra Babu Mokhamatam,[c] Sunil Kumar Manna,[c] Tarun Kanti Mandal[d] and Pulakesh Bera[a,*]

[a]*Post Graduate Department of Chemistry, Panskura Banamali College, Vidyasagar University, Midnapore (E), West Bengal–721152, India*

[b]*Department of Chemistry, CICECO, University of Aveiro, 3810-193 Aveiro, Portugal*

[c]*Centre for DNA Fingerprinting & Diagonostics (CDFD),Hyderabad, Telengana–500 039, India*

[d]*Post Graduate Council, Vidyasagar University, Midnapore, West Bengal –721101, India*

[†] Present address: *Department of Chemistry, Kandi Raj College, Murshidabad, West Bengal, India – 742137*

Abstract

Insertion of acetonitrile in the exocyclic NH_2 group of the thiazole unit of 2-amino-4-(2-pyridyl)thiazole (**HL**) in the presence of copper chloride results in the formation of the monomeric amidine complex [Cu{**L**C(Me)=NH)}Cl_2] (**1**). The same reaction of **HL** and copper(II) perchlorate yields the complex [Cu(**HL**)$_2$]$(ClO_4)_2$ (**2**), without acetonitrile insertion. However, the presence of a spacer donor, e.g. pyrazine, in the reaction medium results in the formation of a dinuclear amidine derivative, [(ClO_4){**L**C(Me)=NH}Cu(μ-pyrazine)Cu{**L**C(Me)=NH}(ClO_4)] $(ClO_4)_2$ (**3**). Complexes **1** and **3** are the first examples of copper assisted iminoacylation of 2-amino pyridylthiazole derivatives, confirming a nitrile to amidine transformation. The new complexes were characterized by single crystal X-ray crystallography, cyclic voltammetry and a DFT study. The complexes have a potential cytotoxic effect in human monocytic cells (U937) with IC_{50} values ranging from 0.84 to 4.5 μM.

ACCEPTED MANUSCRIPT

Significant necrotic activities are ascertained by a lactate dehydrogenase (LDH) enzyme release assay. The interaction with calf thymus (CT) DNA shows the binding constant (K_b) values are ~ 10^4 M^{-1}. The chemical nuclease activity of **1**, **2** and **3** result in 65, 99 and 80% relaxation of supercoiled DNA at 10 μM in the presence of glutathione (GSH, 1 mM), respectively. The study with radical scavengers proved that a hydroxyl or singlet oxygen-like species is responsible for the DNA degradation.

Keywords: Pyridyl-thiazole; Amidine complexes; X-ray crystallography; Cytotoxicity; DNA cleavage

1. Introduction

Thiazoles and their derivatives have recently attracted medicinal chemists because of their biological potential. Compounds containing the 2-amino-1,3-thiazole core occur in many natural products [1–3] and are present in many synthetic products, with a wide range of applications in drug development for the treatment of cancer [4−6], hypertension [7,8], inflammation [9], allergies [10] and bacterial diseases [11]. Proven therapeutic applications of aminothiazole (2-amino-1,3-thiazoles) derivatives has generated a vast area of research in chemistry and biology. In search of bioactive agents, the preparation of 2-amino-1,3-thiazole derivatives is considered as a high throughput research avenue [12]. Li *et al.* reported the syntheses of amino thiazolyl core compounds, showing an interference mechanism on the colchicine binding sites of tubulins, disrupting the microtubule structure of cancer cells [13,14]. Neonicotinoid, a pyridine derivative of aminothiazole, has emerged as an important drug for mammalian α4β2 nAChR and drosophila nAChR because of its high target specificity with relatively low risk for a non-target organism and the environment [15,16]. 2D and 3D model cell cultures were investigated with pyridine-thiazole core compounds to screen for antitumor activity against human breast adenocarcinoma (MCF-7). The results revealed that the pyridine-

ACCEPTED MANUSCRIPT

thiazole compounds are more potent inducers of cell death than cisplatin after a 24 h incubation [17]. Series of substituted 2-(aminopyridyl)- and 2-(aminopyrimidinyl)thiazole-5-carboxamides were identified as potent Src/Abl kinase inhibitors, with excellent antiproliferative activity against hematological and solid tumor cell lines [18]. In search of novel compounds containing the thiazole-pyridine scaffold, we report herein the synthesis of mono and binuclear copper(II) complexes starting from 2-amino-4-(2-pyridyl)thiazole.

In this report, we demonstrate a copper mediated unusual transformation of acetonitrile to an amidine ligand in mono and dinuclear copper(II) complexes, and the cytotoxicity, DNA binding and cleavage activities of the complexes have been studied. To the best of our knowledge, this is a rare example of copper assisted amidine formation of bridged compounds with potential DNA cleavage activity.

2. Experimental

2.1 Materials and methods

2-Acetyl pyridine (99%), thiourea, iodine and pyrazine were obtained from Sigma-Aldrich. Copper perchlorate hexahydrate and copper chloride dihydrate were obtained from Merck chemical company. All solvents (reagent grade) were obtained from commercial suppliers and used after distillation.

*2.2 Synthesis of complex **1***

4-(Pyridin-2-yl)thiazol-2-amine (**HL**) was synthesized following a known method reported earlier [19]. An acetonitrile solution (10 mL) of $CuCl_2.2H_2O$ (1 mmol, 0.172 g) was mixed with

ACCEPTED MANUSCRIPT

an acetonitrile (15 mL) solution of **HL** (1 mmol, 0.177 g). The resulting mixture was refluxed in a water bath for 24 hours. The colour of the solution changed from light yellow to brownish green. The solution was allowed to cool to room temperature. Dark brown crystals separated out upon slow evaporation. Yield: 0.105 g (61.7% based on the metal salt). Elemental analyses (%) for $C_{10}H_{10}Cl_2CuN_4S$: C, 34.02; H, 2.83; N, 15.87; S, 9.07; Found C, 33.99; H, 2.64; N, 15.76; S, 8.89. IR (KBr phase, cm^{-1}): 3335(br), 1634(m), 1515(m), 1377(s), 1115(s), 705(s).

*2.3 Synthesis of complex **2***

The ligand **HL** (1 mmol, 0.177g) was dissolved in 20 ml of methanol, to which a methanolic solution of $Cu(ClO_4)_2.6H_2O$ (1 mmol, 0.243 g) was added . The reaction mixture was then stirred for 1 h at room temperature. The resulting mixture was refluxed in a water bath for 72 h in a 100 mL round bottom flask fitted with a reflux condenser. The color of the solution changed from yellowish green to deep brownish green. The solution was allowed to cool at room temperature. Deep green microscopic crystals separated out on slow evaporation. The crystals were collected by filtration. Yield: 0.168 g (70% based on the metal salt). Elemental analysis (%) for $C_{16}H_{14}Cl_2CuN_6O_8S_2$: C, 31.12; H, 2.26; N, 13.61; S, 10.37; Found C, 30.99; H, 2.24; N, 12.96; S, 9.89. IR (KBr pellet, cm^{-1}): 3450(br), 2106(s), 1601(m), 1520(m), 1353(s), 1139(m), 757(s).

*2.4. Synthesis of complex **3***

An acetonitrile solution of **HL** (1.0 mmol, 0.177 g) was mixed with a methanolic solution of $Cu(ClO_4)_2.6H_2O$ (1.0 mmol, 0.243 g), along with pyrazine (1.0 mmol, 0.08 g). The resulting mixture was refluxed for 72 h in a water bath. The colour of the resulting solution turned to dark brown. The reaction mixture was then filtered and kept at room temperature. Dark-brown

ACCEPTED MANUSCRIPT

crystals were obtained upon slow evaporation. The crystalline product was collected by filtration, washed with acetonitrile and dried. Yield: 0.159 g (65.43% based on metal salt). Elemental analysis (%) for $C_{24}H_{20}Cl_4Cu_2N_{10}O_{16}S_2$: C, 16.66; H, 1.15; N, 8.09; S, 3.70. Found C, 16.29; H, 1.12; N, 7.96; S, 3.64. FTIR (KBr pellet, cm^{-1}): 3446(br), 2354(s), 1610(m), 1525(s), 1377(s), 1115(m), 767(s), 619(s).

2.5 Instrumentation and methods

All density functional theory (DFT) calculation were carried out using the Gaussian 09 program [20]. DFT calculation were performed to locate the stationary points and transition states using the B3LYP and M062x functional with a 6-31g(d) basis set. Another calculation was carried out using the B3LYP functional with a def2svp basis set. The structure of the stationary point or the transition state was confirmed by frequency calculations at the same level theory. Intrinsic reaction coordinate (IRC) calculations were performed to confirm the connection of each transition state to its corresponding reactant and product. All structures of reactants and products from the IRC calculations were further optimized at the same level and their structure and energy compared with their corresponding transition state. The reported Gibbs free energies (ΔG) and enthalpies (ΔH) are all in the gas phase at 298 K. M062x was used in the calculations to include dispersion energies, though it showed a similar potential energy surface as the B3LYP functional. Cyclic voltammetric experiments were performed at room temperature in anhydrous acetonitrile solvent using tetra butyl ammonium perchlorate as the supporting electrolyte on a CH Instrument electrochemical workstation model CHI630E. The conventional three-electrode assembly was comprised of a platinum working electrode, a platinum wire auxiliary electrode and Ag/AgCl reference electrode. UV-Vis absorption spectra of the samples were recorded on a Perkin Elmer Lambda 35 spectrophotometer in the wavelength range 200-800 nm at room

ACCEPTED MANUSCRIPT

temperature. The FTIR analyses (400-4000 cm^{-1}) were performed by using a Perkin Elmer USA, Frontier FT-IR/FIR spectrometer. The samples were prepared as KBr pellets using anhydrous KBr salt. Single crystal X-ray diffraction data for the ligand and the complexes were collected with monochromated Mo-Kα radiation (λ = 0.71073 Å) on a Bruker Kappa Apex-II diffractometer, equipped with a CCD area detector at low temperatures. Several scans in φ and ω directions were made to increase the number of redundant reflections and were averaged during the refinement cycles. Data processing for all the complexes were performed using the Bruker Apex-II suite. Reflections were then corrected for absorption, inter-frame scaling and other systematic errors with SADABS [21]. All the structures were solved by direct methods and all non-hydrogen atoms were refined anisotropically by full-matrix least squares based on F^2 using SHELXL-97 [22].The hydrogen atoms were isotropically treated using a riding model with the isotropic displacement parameters depending on their parent atoms. The molar conductance of 10^{-3} (M) solutions of the metal complexes in DMSO were measure at 30 °C using a Thermo Orion model 550A conductivity meter and a dip-type cell with a platinized electrode. The elemental analyses (C, H, N and S) of the complexes were performed using a FISONS EA-1108 CHN analyzer.

2.6. In vitro biological studies

2.6.1. MTT assay

The cytotoxicity of complexes **1**–**3** were assessed using an MTT (3-(4,5-dimethylthiazol-2-yl)-2,5-diphenyltetrazolium bromide) assay based on the ability of mitochondrial dehydrogenase in viable cells to transform the tetrazolium ring of MTT, forming dark blue membrane-impermeable crystals of formazan that could be measured spectrophotometrically.

ACCEPTED MANUSCRIPT

The amount of formazan product is a measure of the viable cells. About 5000 cells/well of human lymphoma cells (U937) were seeded in a 96 well plate and treated with different concentrations of the ligand (L) and the copper compounds **1**–**3**. After 72 h of incubation of the samples in a CO_2 incubator, 20 μL of MTT dye (5 mg/mL in PBS) were added per well, and incubation was continued for 3 h at 37 °C. The culture medium was discarded and 100 μL of lysis buffer (20% SDS in 50% dimethylformamide) were added and kept for 1 h on a shaker to solubilize the cell membrane and dissolve the formazan crystals. The absorbance at 595 nm was determined using an ELISA microplate reader. The cytotoxicity of the test compounds was measured as the percentage ratio of the absorbance of the treated cells over the untreated controls. The IC_{50} values were determined by non-linear regression analysis using the Graphpad prism software [23].

2.6.2. Lactate dehydrogenase (LDH) release assay

LDH, a cytosolic enzyme, is usually leaked out along with cytosolic contents upon induction of cell necrosis. U937 cells were treated as stated earlier in the cytotoxicity assay experiment. The culture supernatants were collected and the LDH activity was assayed after 20 minutes incubation at 25 °C with a substrate solution (30 mM sodium pyruvate and 6.6 mM NADH in 0.2 M Tris-Cl, pH 7.3). The absorbance at 340 nm was measured. The LDH activity was indicated as the relative cytolysis of the compound treated cells from a plot considering absorbance of triton X-100 treated cells as 100%.

2.6.3. Binding studies with CT DNA

For CT DNA binding activity experiment, a stock solution of CT-DNA was prepared in 50 mM Tris-HCl/50 mM NaCl in H_2O at pH 7.4. To exclude free protein in the CT DNA, the

ACCEPTED MANUSCRIPT

UV absorbance experiment was carried out in a buffer medium of CT DNA and the ratio of absorbance found at 260 and 280 nm was *ca.*1.9:1, which suggests that the CT DNA was apparently free from protein. The stock solution of DNA was stored at 4 °C and used within five days. The molar concentration of the stock solution in base pairs was calculated using a molar absorption coefficient value of 6600 M^{-1} cm^{-1} at 260 nm and adjusted to 5 mM concentration. The interaction of the Cu(II) complexes **1-3** with CT DNA was carried out using the UV−Vis spectroscopic titration method in 5 mM Tris-HCl buffer (pH=7.2) at room temperature. The complex solution was also prepared in the same medium. The concentration of complexes **1**−**3** for this titration was fixed to 40 μM. The change in the absorbance was recorded with the subsequent addition of an aliquot of 6 μL (concentration of 5 x 10^{-3} M) CT DNA in the sample and reference cuvette. All the UV spectra were recorded after equilibration of the solution for 5 min. The experiment was continued until there was no significant change in absorbance for the last four successive additions [23].

2.6.4. DNA cleavage experiments

Cleavage of supercoiled pEGFP-C3 (4.7 kb) DNA (0.4 μg, 4727 base pairs) was studied by agarose gel electrophoresis using the metal complexes in 50 mM tris(hydroxymethyl)-methane-HCl (Tris-HCl) buffer (pH 7.2) containing 50 mM NaCl. The chemical nuclease activity of the complexes was studied using hydrogen peroxide (200 μM) as the oxidizing agent and glutathione (GSH, 1 mM) as the reducing agent. Each sample was incubated for 1.0 h at 37 °C and analyzed for the cleaved products using gel electrophoresis following the procedures reported earlier [24−27]. The extent of the DNA cleavage was calculated from the intensities of the bands using the UVITEC Gel Documentation System. Due corrections were made for the low level of the nicked circular form present in the original supercoiled DNA sample and for the

ACCEPTED MANUSCRIPT

low affinity of EtBr binding to supercoiled compared to the nicked circular and linear forms of DNA. The concentrations of H**L** and **1-3** (10 μM) corresponded to that in the 20 μL final volume of the sample using Tris buffer. Mechanistic studies were performed using inhibitors of reactive oxygen species (ROS), such as DMSO and glycerol (hydroxyl radical scavengers), sodium azide and histidine (singlet oxygen scavengers) and catalase (peroxide radical inhibitors).

3. Result and discussion

3.1. Acetonitrile insertion

Scheme 1 shows the synthesis of the copper(II) complexes from 2-amino-4-(2-pyridyl)thiazole (H**L**). In our experiment, the insertion of CH_3CN with the exocyclic amine group of H**L** occurs in the presence of copper(II) chloride upon prolonged heating in excess acetonitrile. Absence of the copper(II) ion did not lead to the said transformation. However, the reaction of $Cu(ClO_4)_2$ and H**L** in excess CH_3CN did not result the amidine formation, but a complex with the composition $[Cu(L)_2](ClO_4)_2$ was obtained on prolonged refluxing. Interestingly, the addition of a spacer molecule (pyrazine) to the mixture of $Cu(ClO_4)_2$ and H**L** furnished the dinuclear amidine complex **3**. Higher concentrations of CH_3CN in the reaction medium leads to coordination of CH_3CN to the copper(II) centre, along with H**L** satisfying the secondary valence of copper. From a chemistry point of view, the exocyclic amine group of the thiazole ring in the pyridine–thiazole compound is susceptible to make bonds with electron deficient small groups, like molecular oxygen [28], carbon dioxide [29−32], acetonitrile [33−35] etc. The preparation of amidine compounds has a high interest due to their versatile synthetic utility in organic [33], medicinal [34] and coordination chemistry [35]. The direct synthesis of an amidine from a nitrile can only be achieved when the latter is activated by a strong electron acceptor group. For instance, Longato *et al.* performed the insertion of acetonitrile into the exocyclic amine group of

ACCEPTED MANUSCRIPT

deprotonated nucleobases, e.g. 9-methyl adenosine (9-MeAd) and 1-methyl cytosine (1-MeCy), when a mixture of *cis*-$[L_2Pt(\mu\text{-oxa})]_2(NO_3)_2$, 9-MeAd and/or 1-MeCy with CH_3CN was reacted at RT [36]. Keppler reported for the first time the Ru(II) mediated acetonitrile addition to 1-indazole [37]. In another report, Moise *et al.* reported the acetonitrile insertion to tris (2-aminoethyl) amine (*tren*) during complexation with $AlMe_3$ [38]. Acetonitrile was observed to undergo an interesting oligomerization in the system; each primary amine linkage of *tren*, i.e. $-CH_2CH_2NH_2$, was extended to $CH_2CH_2NHC(Me)NC(Me)NH_2$ by the coupling of two molecules of CH_3CN. This unique cyclization of CH_3CN is assumed to be mainly due to reduction of the electronic charge of the carbon-nitrogen triple bond [39]. However, transformations of acetonitrile to amidine compounds are not so numerous [40]. The influence of precoordinated ligands, such as DMSO, PPh_3 or $PMePh_2$, facilitated the formation of amidine complexes, which were stabilized by several steric and electronic factors [24, 30].

ACCEPTED MANUSCRIPT

ACCEPTED MANUSCRIPT

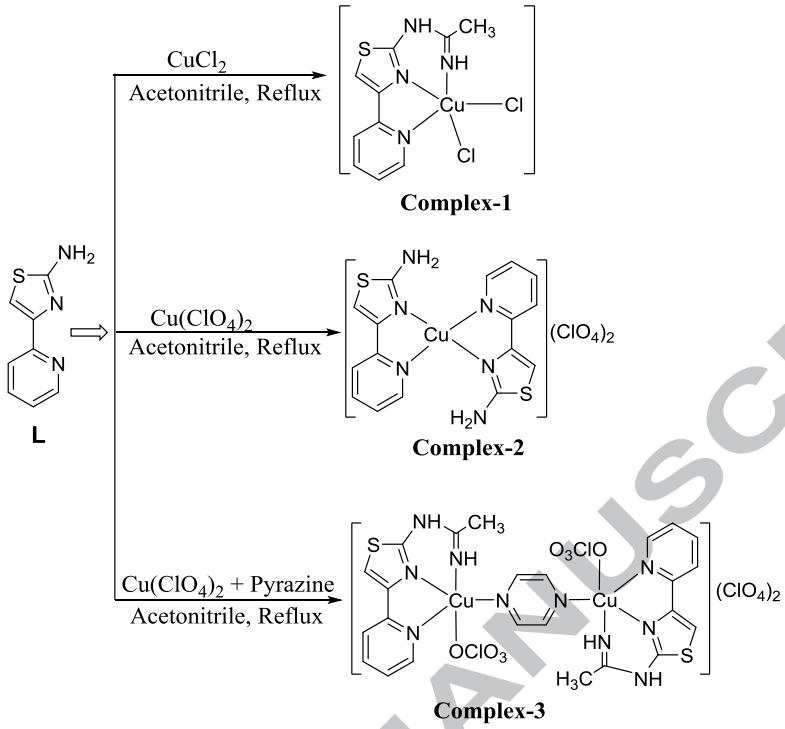

Scheme 1**:** Synthesis of complexes **1**–**3**.

It was suggested that the coupling reaction proceeded through coordination of the nitrile to the metal centre of the precursor complex, followed by intramolecular nucleophilic addition of the amine ligand. Iminoacylation occurred when moderate to strong π–acceptor ligands, such as DMSO and CO, were positioned in the *trans* position to the coordinated CH_3CN ligand in the coordination sphere [24,30,41]. In the present case, the coordination of CH_3CN through the N atom to the copper atom reduces the electron density on CN, which increases the electrophilicity of the C atom of CH_3CN. The adjacent heterocycle exocyclic NH_2 group of H**L** gains sufficient nucleophilicity due to conjugation in the ligand molecule and so can attack the electron deficient C atom of CH_3CN. Additional stabilization in the system arises from the chelate effect that is attributed to the formation of an extra six membered chelate ring. This amidine complex

ACCEPTED MANUSCRIPT

formation is a metal assisted process *via* formation of a CH_3CN coordinated transition state, as shown in Scheme 2.

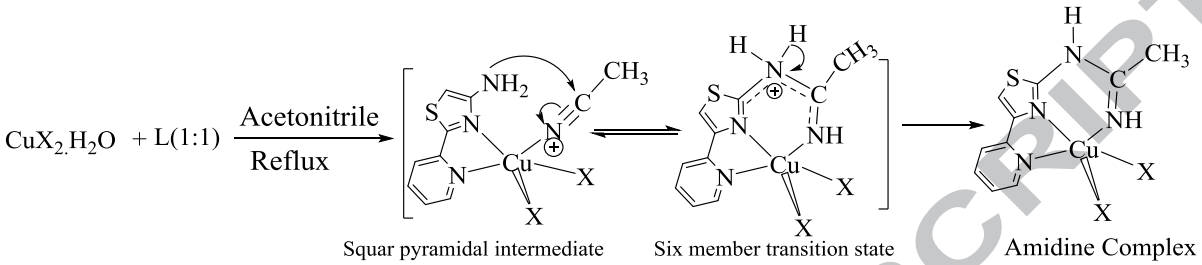

Scheme 2**:** Mechanism of CH_3CN insertion is the formation of the amidine complex.

To support the mechanism of a metal assisted coupling reaction of CH_3CN with **HL** and the subsequent formation of amidine complexes **1** and **3**, DFT (density functional theory) calculations were carried out using the B3LYP and Mo6Lx functional with a 6-31G(d) basis set [42,43,44]. To understand the role of the metal in the CH_3CN addition to **HL**, the CH_3CN coordinated [Cu(CH_3CN)HL] model complex was taken as a starting point (Figure 1a).

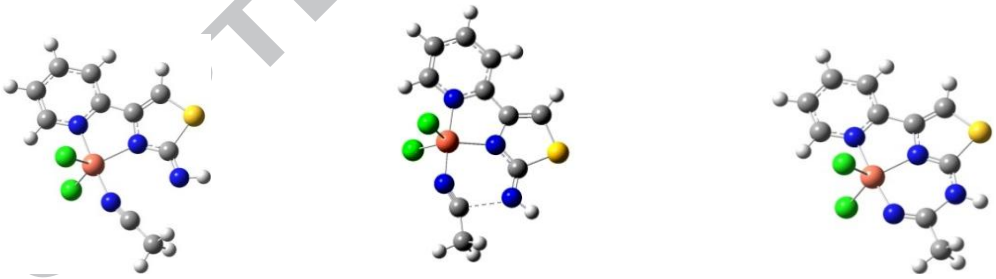

Reactant Transition State (TS) Product

Figure 1(a). Model reactant, transition state and product in metal assisted acetonitrile insertion.

ACCEPTED MANUSCRIPT

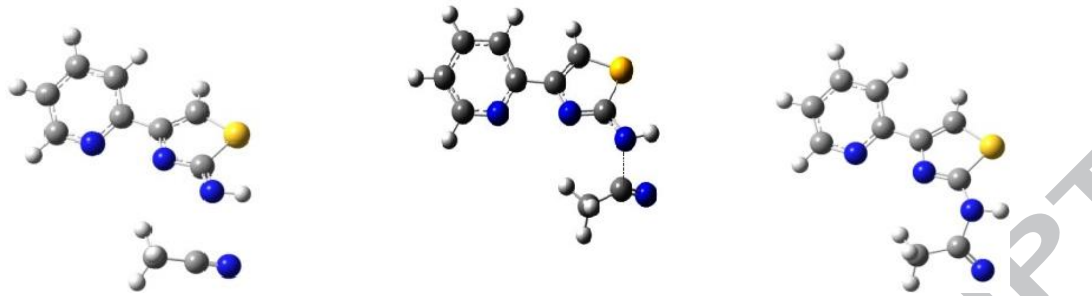

Reactant Transition State (TS) Product

Figure 1(b). Model reactant, transition state and product without metal in the reaction of L and acetonitrile.

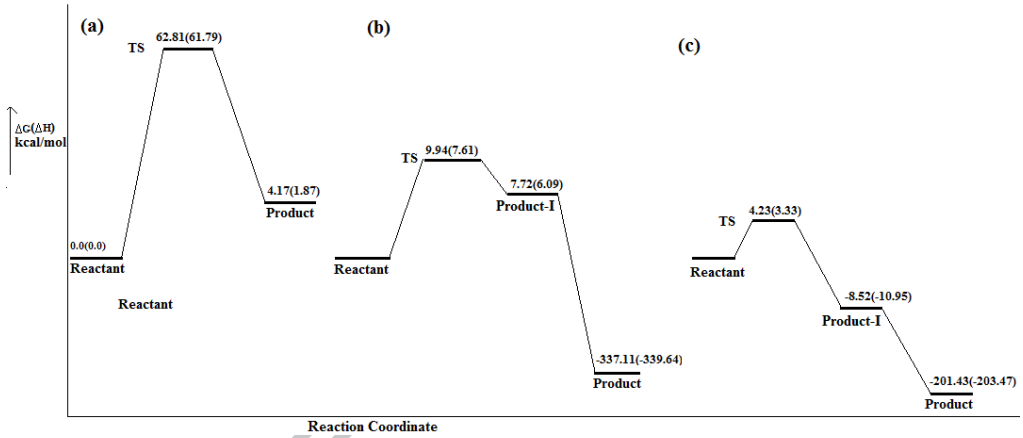

Figure 2. DFT computed potential energy surface of (a) the non-catalyzed reaction (b) the Cu-catalyzed reaction of chloride complex and (c) the Cu-catalyzed reaction of the pyrazine bridged complex

A comparison with the model system without copper was also considered in this respect (Figure 1b). The modelled stationery points and the transition states were confirmed by frequency calculations at the same level of theory (Figure 2). Intrinsic reaction coordinate (IRC) calculations confirmed the hypothetical connection of the reactant and product in the transition state. The calculated free energy in the metal assisted CH_3CN coupling with L has a greater value (20.59 kcal/mole) than the free energy of the transition state without the metal (13.39

ACCEPTED MANUSCRIPT

kcal/mol). The values are given in Tables S1−S3 and the respective transition states are shown in Figures S1 to S3. This result reveals that the transformation of the nitrile to the amidine complex occurs *via* CH_3CN coordination to the copper centre.

The complexes were also characterized by conductance measurements, UV-Vis and infrared (IR) spectroscopy, as shown in Figures S4–S10 in the supplementary material. Complexes **2** and **3** are 1:2 electrolytes in DMF, giving molecular conductance values of 221 and 212 $\Omega^{-1}cm^2\,M^{-1}$ at 25 °C, respectively. The low molar conductance value of **1** (11 $\Omega^{-1}cm^2\,M^{-1}$) demonstrates its neutral monomeric nature in DMF solution at 25 °C. The high intensity excitonic peak near 310 nm in the UV-Vis spectrum of L (Fig. S4) and the complexes (Figs. S5–7) is obtained due to a charge transfer transition. The coordination mode of the ligand was supported by a comparison of some characteristic vibrational peaks of the ligand to that of the complexes. The IR spectra of the complexes (Figs. S8–S10) show broad bands in the range 3000−3500 cm^{-1}, which can be assigned to the stretching vibration of the NH/NH_2 bonds and the extended hydrogen bonding in the solid state of the complexes. The IR spectra of **1** and **3** display strong stretching vibrations at 1634 and 1610 cm^{-1}, corresponding to the amidine system arising from the thiazolyl amine-acetonitrile coupling [11]. The characteristic C=N (pyridyl) stretching frequency of the complexes was observed at ca. 1525 cm^{-1}. The stretching vibration frequency of the Cl−O bonds in the IR spectra of **2** and **3** was observed at 1115 cm^{-1}, while the corresponding bending vibrations were obtained at 610 cm^{-1} for **2** and 619 cm^{-1} for **3**. The splitting of ν_{Cl-O} (stretching) in the spectra may result from the involvement ClO_4^- in hydrogen bonding within the crystal lattice [45].

3.2. Electrochemistry

ACCEPTED MANUSCRIPT

The reduction and oxidation peaks values of **2** and **3** are given in Table 1. The cyclic voltammogram of **2** has three reduction peaks at –0.738 (A), 0.29 (B), and 0.93 V (C) versus an Ag/AgCl standard calomel electrode and oxidation peaks at 0.845 (D) and 1.049 V (E) versus an Ag/AgCl standard electrode (Figure S11a). Similarly, the cyclic voltammogram of complex **3** shows four reduction peaks at –0.54 (A′), –0.13 (A″) +0.19 (B′) and +0.89 V (C′) versus Ag/AgCl, while there are two oxidation peaks at +0.84 (D′) and +1.12 V (E′) versus Ag/AgCl, saturated KCl at a scan rate 100 mVs^{-1} (Figure S11b). The peaks at A in **2** and A′, A″ in **3** correspond to the reduction of the organic molecule, e.g. the pyrazine and thiazole rings. The reduction peaks at B and C in **2** and B′ and C′ in **3** occur in the same potential ranges, which reveals the reduction of the same kind of metallic species. The reduction peaks at B or B′ and C or C′ may be attributed to the reduction of Cu(II) to Cu(I) and Cu(I) to Cu(0) species, respectively. The oxidation peak in the anodic scan at 0.84 V corresponds to the oxidation of Cu(I)→Cu(II) and the remaining oxidation processes, i.e. Cu(0)→Cu(I). The reduction and oxidation processes are irreversible in nature, which reveals that the electrolyte predominantly forms one kind of species [46]. However, for the entire redox event the oxidation peak height is much less than the reduction peak height. Multiple reduction peaks originating from the reduction of heterocyclic rings of the ligand might be beneficial for a good DNA interactive molecule [47].

Table 1.

Reduction and oxidation potentials of complexes **2** and **3**.

	Reduction process (in volts)			Oxidation process (in volts)	
Complex	Reduction of organics	$Cu^{II} \rightarrow Cu^{I}$	$Cu^{I} \rightarrow Cu^{0}$	$Cu^{I} \rightarrow Cu^{II}$	$Cu^{0} \rightarrow Cu^{I}$
2	–0.738 (A)	0.29 (B)	0.94 (C)	0.84 (D)	1.09 (E)

ACCEPTED MANUSCRIPT

3	–0.54 (A′) –0.13 (A″)	0.19 (B′)	0.89 (C′)	0.84 (D′)	1.11 (E′)

3.3. X-ray crystallography

Perspective views of complexes **1**–**3** are shown in Figures 3, 4 and 5, respectively. Crystal refinement data of the complexes are listed in Table 2 and selected bond angles and bond distances are given in Tables S4 and S5 (see Supplementary Information).

Table 2:

Crystal parameters of complexes **1**, **2** and **3.**

Parameter	**1**	**2**	**3**
CCDC	1532570	1532571	1532572
Empirical formula	$C_{10}H_{10}Cl_2CuN_4S$	$C_{16}H_{14}Cl_2CuN_6O_8S_2$	$C_{24}H_{20}Cl_4Cu_2N_{10}O_{16}S_2$
Fw, g/M	352.73	616.89	1037.50
Crystal system	monoclinic	orthorhombic	triclinic
Space group	*P21/c*	*Pbca*	*P -1*
a (Å)	10.0018(7)	15.9967(9)	7.8954(3)
b (Å)	8.4480(6)	15.3037(9)	14.3371(5)
c (Å)	14.6636(10)	17.8805(11)	16.6680(6)
α (°)	90	90	108.101(1)
β (°)	95.956	90	103.275(1)
γ (°)	90	90	93.247(1)
V (A^3)	1229.88(15)	4377.3(4)	1728.69(11)
Z	4	8	4
T (K)	150	150	150
σ calcd, g cm^{-3}	1.905	1.872	1.993
λ, Å (Mo Kα)	0.71073	0.71073	0.71073
μ (mm^{-1})	2.364	1.493	1.752
F (000)	708.0	2488.0	1040.0
Goodness-of-fit	0.993	0.997	0.994
R (wR)	0.0334 (2040)	0.0477 (3374)	0.0443 (7291)

Complex **1** crystallizes in the monoclinic space group P21/c and consists of a neutral molecule of [Cu{LC(Me)=NH)}Cl_2] (Figure 3). The copper atom is coordinated axially by one chloro ligand [Cu–Cl1, 2.6363(9) Å] and equatorially by another chloro ligand [Cu–Cl2,

ACCEPTED MANUSCRIPT

2.2430(9) Å] and an NNN donor formed *via* coupling of acetonitrile with **HL**. The CuN_4Cl_2 ligand sphere adopts a square pyramidal structure with a τ value of 0.096. Chelation of the copper centre by the new amidine ligand is reflected in the Cu–N2 and Cu–N4 distances of 1.953(2) and 1.976(2) Å. A somewhat shorter hydrogen bonding distance (2.275 Å) is observed for the amidine nitrogen atom. The crystal packing of **1** is stabilized by strong $\pi\ldots\pi$ stacking and hydrogen bonding interactions (Figure S12); interestingly alternate layers are formed in the crystal lattice through the hydrogen bonding and $\pi\ldots\pi$ stacking. In addition, there is hydrogen bonding between the N3–H hydrogen atom of one molecule and the bonded Cl atom of another molecule and π–π stacking involves the two π electronic systems of the pyridine and thiazole rings.

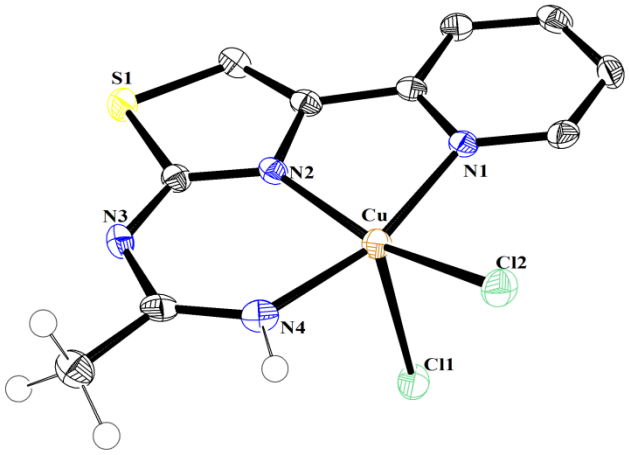

Fig 3. Molecular structure of complex **1**. Thermal ellipsoids are drawn at the 50% probability level.

Complex **2** crystallizes in the orthorhombic space group Pbca with one complex cation and two distorted perchlorate ions. In the cationic unit, the copper(II) ion is coordinated to the ligand molecule (L) through the pyridinyl and thiazolyl ring nitrogen atoms (Figure 4). Four of

ACCEPTED MANUSCRIPT

the donor nitrogen atoms and the central copper(II) ion are in an approximate square planar arrangement with a τ value of 0.09 [48,49]. According to Reedijk and Adison, a τ value of zero represents a perfect square pyramidal structure while τ = 1 represents a perfect trigonal bipyramid geometry. The average Cu–N distance is 1.9775(3) Å. The out of square plane Cu–N bond distance is slightly higher (0.03Å) than the average Cu–N bond distance. An adjacent coordinate unit forms a linear structure through the bridged perchlorate anion.

A detailed analysis of the hydrogen bonding interactions in complex **2** (Table S6) shows the existence of a 2D N–H···O network of hydrogen bonds between the N3 and N6 atoms with oxygens atoms from both perchlorate ions. As in complex **1**, there are π···π interactions between the pyridinyl rings of adjacent molecules, characterized by an inter-planar distance of 3.682 Å and a shift distance of 1.417 Å.

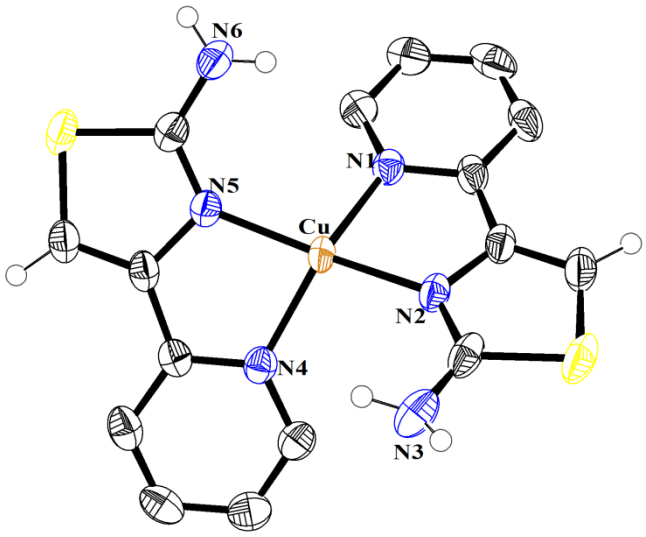

Fig 4. Molecular structure of complex **2**. Thermal ellipsoids are drawn at the 55% probability level. The structure is truncated to highlight the ligand-metal binding geometry

ACCEPTED MANUSCRIPT

The dinuclear complex [(ClO_4){**L**C(Me)=NH}Cu(μ-pyrazine)Cu[{**L**C(Me)=HN}(ClO_4)](ClO_4)$_2$ (**3**) crystallizes in the centrosymmetric triclinic P1 space group. The asymmetric unit contains a bicopper unit bridged by a pyrazine ligand, two amidine ligands and four perchlorate anions, of which two are coordinated to the copper atoms (Figure 5). The complex cation of **3** is formed by a pyrazine bridged Cu^{II} dimer, and the two copper atoms are related to each other through an inversion centre which is located at the centre of the pyrazine ring that bridges the two copper centers in an end on fashion. The Cu…Cu bond distance is 6.859 Å, giving sufficient room for the perchlorate ions to approach along the axial position to the copper(II) atoms. Charge neutralization is ensured by the presence of the two symmetrically related perchlorate counter ions in respect to the centrosymmetric cationic part of **3**. The geometry of the metal centres can be best described as square pyramidal. The four corners of the square are occupied by three nitrogen atoms of the amidine ligand and one nitrogen atom of the bridging pyrazine ring. The oxygen atom of a perchlorate anion occupies the axial position of the square pyramid. The two amidine ligands and two perchlorate ions arrange themselves *trans* to each other with respect to the pyrazine bridged ring. The Cu–N bond distances fall in the range 1.948(3) to 2.035(3) Å, which is very similar to the range of Cu–N bond distances for published copper(II) complexes [50−52]. The crystal packing of **3** is stabilized by the strong electrostatic force of attraction between the +2 charge of the complex cation and the ClO_4^- anions, and interestingly they formed alternate layers of complex **3**, as depicted in the crystal packing diagram presented in Figure S13. No classical hydrogen bonds are observed in the structure of **3**.

ACCEPTED MANUSCRIPT

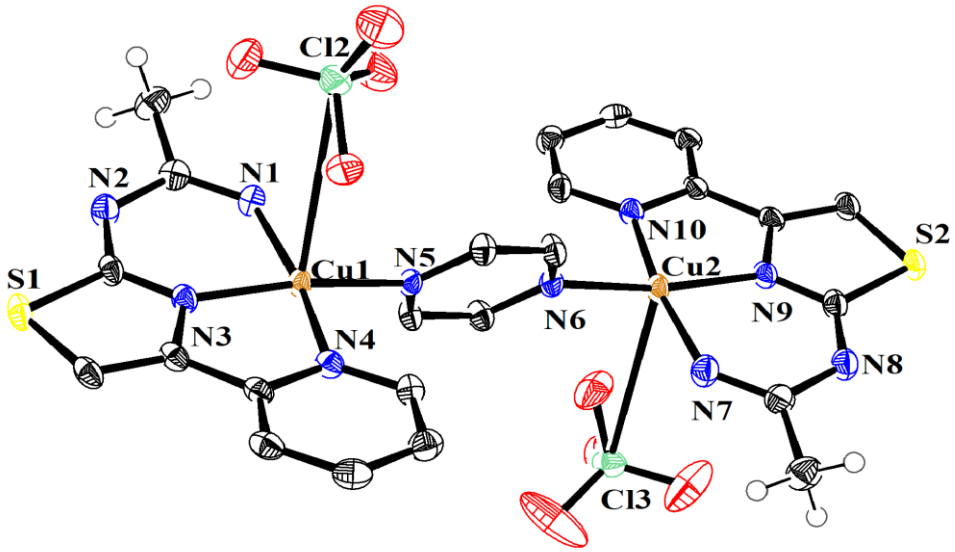

Fig 5. Molecular structure of complex **3**. Thermal ellipsoids are drawn at the 55% probability level. Structure truncated to highlight the insertion of acetonitrile in the ligand-metal binding geometry.

3.4 Biological study

3.4.1. Cytotoxicity assay

U937 human monocytic cells were treated with the ligand 2-amino-4-(2-pyridyl)thiazole (**HL**) and complexes **1**–**3** to probe their *in vitro* cytotoxicity using an MTT cytotoxicity assay **(**Figure S14**)**. The ligand is not cytotoxic against the U937 human monocytic cell line (Figure 6A). However, the copper derivatives of the **HL** are quite potent in inhibiting cell proliferation, showing IC_{50} values ranging from 0.84 µM to 4.5 µM. A control experiment for the MTT assay using normal peripheral blood mononuclear cells (PBMC) was performed. The compounds did not show any significant toxicity in the PBMCs (Figure S15). In this context, it can be noted that the ligand (**HL**) has no cell cytotoxicity effect, unlike the copper complexes **1**−**3**, suggesting that

ACCEPTED MANUSCRIPT

the copper centre has a specific tendency to accumulate in the cell cytoplasm. Complex **3** is the most potent compound, with an IC_{50} value of 0.45 ± 0.6 μM (Figure 6D), and complex **2** is the least potent, with an IC_{50} value of 3.7 ± 0.3 μM (Figure 6C). Complex **1** shows an intermediate potency, with an IC_{50} value of 0.8 ± 0.1 μM (Figure 6B). Such a variation in activity appears to be dependent on structural changes and acetonitrile insertion in the compound **HL**. The non-planar nature of the ligand with a sulfur atom may induce an electrostatic interaction in DNA. The highest cytotoxic effect of **3** may be attributed to the highest hydrophobicity of the crowded copper(II) centres within the pyrazine bridged dicopper(II) complex among the reported complexes. It can safely be concluded that copper(II)-amidine compounds, e.g. **1** and **3**, have a higher cytotoxicity effect than the corresponding non-amidine compound, e.g. **2**.

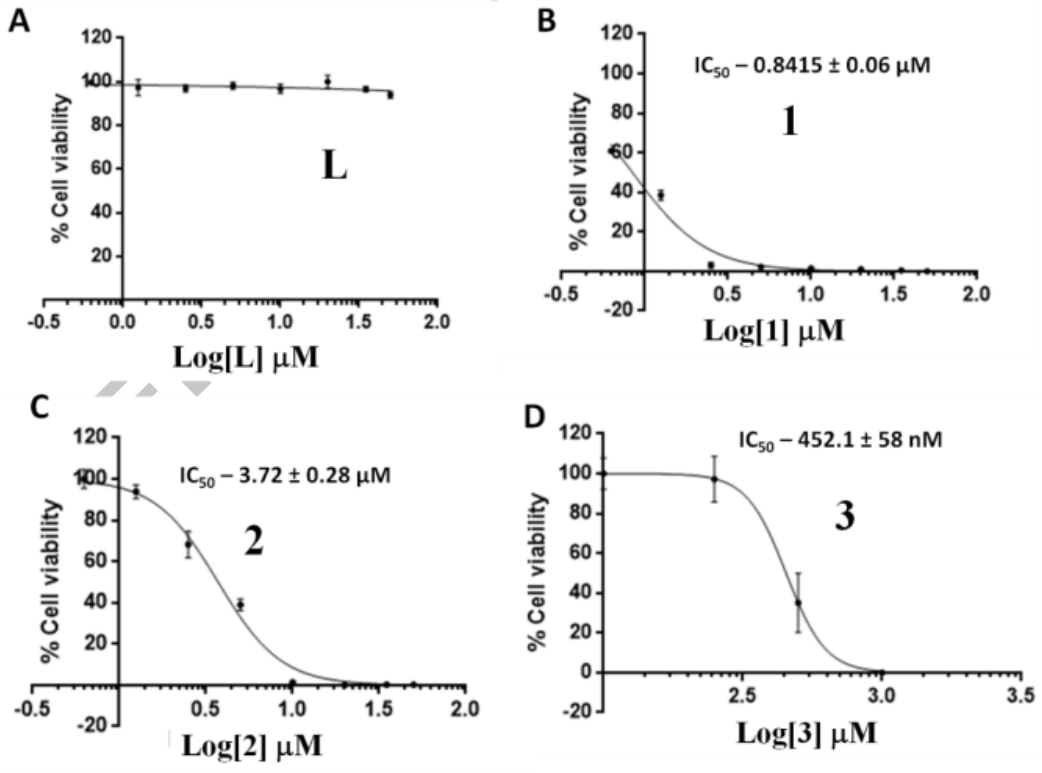

Fig 6 Cytotoxicity effect of the compounds on U937 cells. U937 cells were treated as shown above for 72 h, with different concentrations of (A) the ligand **HL**, (B) **1**, (C) **2**, (D) **3**, an MTT

ACCEPTED MANUSCRIPT

assay was done and the percentage (%) of cell viability was plotted. Data were transformed, normalized and IC50 values were calculated using Graph pad Prism. Data represents mean ±SD of three independent experiments.

3.4.2. Assay for cytolysis

An LDH assay was employed to differentiate the apoptotic (programmed cell death) activities of these reported compounds from their necrotic activities. **HL** did not show any significant cytolysis, even at a 50 μM concentration. The copper complexes **1**–**3** caused significant cytolysis (Figure 7). The data suggest that complexes **1**, **2** and **3** are likely to follow an apoptosis (as cytolysis is less than 40%) path for programmed cell death [53]. However, **1** demonstrates both apoptotic and necrotic pathways (as cytolysis is nearly equal to 40%). So, **2** and **3** can be used as better drugs than **1** in cancer treatment.

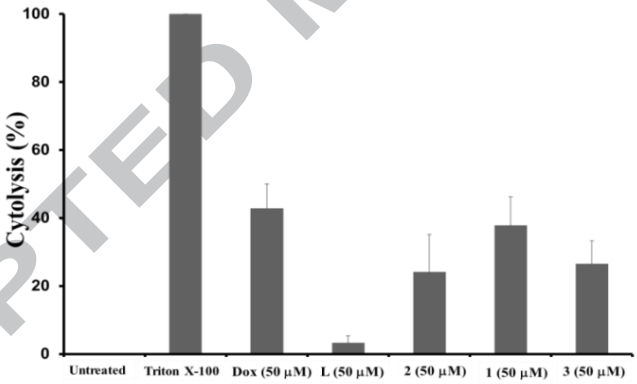

Fig 7. LDH release assay on cytolysis of U937 cells with **HL** and complexes **1**–**3**. U937 cells were treated for 24 h with 50 μM of the different compounds in DMSO solvent and 5 μM of doxorubicin as a positive control. LDH release was plotted as a percentage against triton X-100, which is considered as 100% and untreated cells were considered as 0% and the vertical line on each bar represents mean ±SD of three independent experiments.

3.4.3. DNA binding study

ACCEPTED MANUSCRIPT

Intercalation of any complex involves the strong stacking of planar aromatic rings of a coordinated ligand(s) with the base pair of CT DNA. The binding usually remits a hypochromic red shift of the ligand [54]. The extent of the hypochromism generally indicates the drugs intercalative binding strength. The intensity of the absorption of the complex-DNA system leads to a decreased intensity at around 235 and 310 nm (Figure 8). The change of absorption values at 308 nm (for **1**), 316 nm (for **2**) and 307 nm (for **3**) in the complex-DNA system were used to calculate the binding constant (K_b). The binding constant (K_b) is calculated from the spectroscopic data using the known equation, $[DNA]/|(\varepsilon_a-\varepsilon_f)|=[DNA]/|(\varepsilon_b-\varepsilon_f)|+I/k_b|(\varepsilon_b-\varepsilon_f)|$ where [DNA] is the concentration of DNA, $\varepsilon_a = A_{obsd}/[complex]$, ε_f = the excitation coefficient for the free (unbound) complex and ε_b = the extinction coefficient for the complex in the fully bound form. A plot of $[DNA]/(\varepsilon_b- \varepsilon_f)$ vs [DNA] gives a slope of $[1/(\varepsilon_b- \varepsilon_f)]$ and an intercept of $[1/K_b(\varepsilon_b- \varepsilon_f)]$; thus the K_b value is found from the ratio of the slope to the intercept, as shown in Figure S16. The K_b values of the complexes are in the order **2** (34.11×10^3) > **1** (4.66×10^3) > **3** (4.52×10^3). The greater K_b value of complex **2** indicates a greater binding to DNA than the other two copper thiazole-pyridine compounds [55].

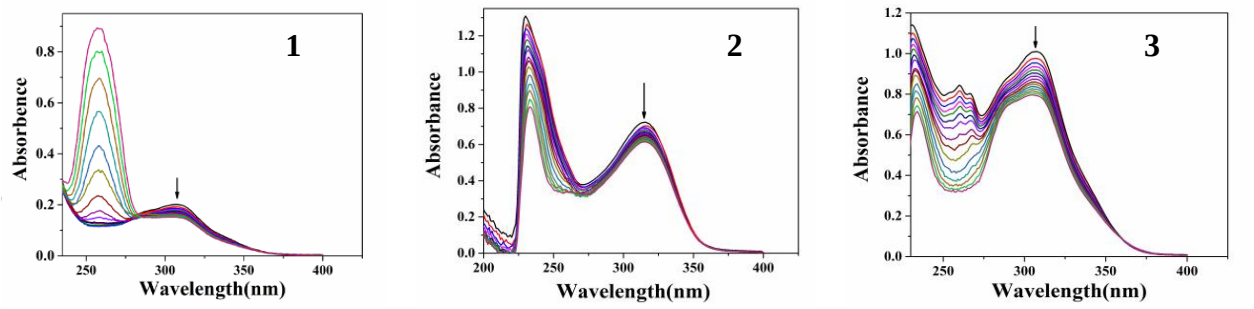

Fig 8. Absorption spectra of complexes **1**, **2** and **3** in Tris-HCl/NaCl buffer with increasing DNA concentration (shown by the arrowhead)

3.4.4. DNA cleavage activity

ACCEPTED MANUSCRIPT

Figure 9 shows the results of the gel electrophoresis separation of pEGFP-c3 (4.7 kb) DNA induced by the compounds. The ligand **HL** did not show any chemical cleavage activity under both reducing and oxidizing conditions (Figures 9A and 9B, lane 4). In contrast, the copper complexes **1**–**3** exhibited about, 65, 99 and 80% DNA cleavage activity, respectively, in the reducing environment (Figure 9A, lanes 6, 5 and 7). Compounds **1**−**3** did not show any appreciable DNA cleavage activity in the oxidizing environment (Figure 9B, lanes 6, 5 and 7). Such variations in activity appear to be dependent on the nuclearity of the structure. A double strand junction may uniquely offer the proximity of two DNA strands to assemble with the copper complex for interaction. The significant gain in potency in **1** and **3** can be realized by the amidine complex formation of **HL**. The derivative that was obtained from the insertion of acetonitrile in the thiazole ligand blocked migration and invasion of cancer cells by impairing the cytoskeleton dynamics accompanied by reduced co-localization. The efficiency of the DNA oxidation is also sensitive to incremental changes in the flexibility of the target sequences. Each multinuclear complex investigated to date has shown a unique dependence on the nucleotide sequence surrounding its target junction [17, 54, 55]. This type of dependence is typically indicative of metal-purine or metal-guanine coordination. The chemical nuclease activity of the Cu^{II} complexes is also known to be better in the presence of external activators, *viz.* ascorbic acid, glutathione or hydrogen peroxide (H_2O_2), and may proceed through different mechanistic pathways. The axial coordination, occupied by the perchlorate oxygen atoms, of the amidine complex **3** is highly labile in nature due to Jahn-Teller distortion in the d^9 system. Hence the longer Cu–O bonds may be susceptible to dissociation during the redox reaction in the presence of glutathione and O_2, which promotes the binding of molecular oxygen to the reduced Cu(I) centre. The excellent cleavage activity (80%) might be due to the preferential binding of

ACCEPTED MANUSCRIPT

molecular oxygen with the reduced form of copper in its +1 state. This binding effect is likely to be more active in the generation of reactive oxygen species for DNA cleavage activity. Further, the long Cu–Cu distance (6.858 Å) in the dinuclear complex **3**, which is one third of the helix diameter (20 Å), may help **3** to intercalate effectively between the DNA base pairs. The intercalated form of the phosphodiester backbones of nucleic acid DNA thus facilitates the cleavage performance. A similar mechanistic pathway may be applicable to **1**, which shows 65% DNA cleavage activity under the experimental conditions. The highest chemical nuclease activity (99%) among the reported compounds is shown by the mononuclear non-amidine compound **2**. The quasi planar complex (**2**) has sufficient vacant space in the coordination site to bind with molecular oxygen to the reduced Cu(I) centre, facilitating the generation of ROS for the DNA cleavage activity more than the bridged dimeric copper(II) complex. Besides, the DNA may uptake **2** more through certain receptors due to presence of sulfur and free amine functions in its structure [56]. It can be safely concluded that the less crowded square planar copper(II) centre in **2** is more active for DNA cleavage than the crowded five coordinated copper(II) centre(s) of **1** and **3**.

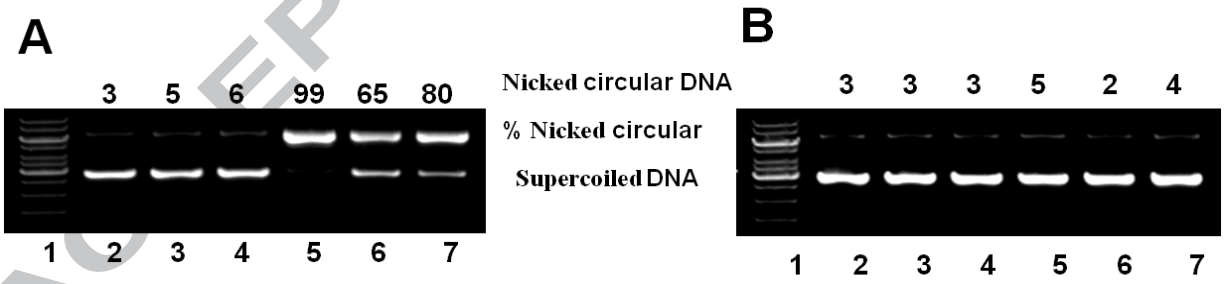

Fig 9. Different copper compounds (10 µM) were incubated with 400 ng of pEGFP-C3 DNA for 2 h at 37 °C, either in a reducing environment consisting of 1 mM of reduced glutathione (A) or an oxidizing environment consisting of 200 µM of H_2O_2. Figure A: lane 1 (1 kb DNA marker), lane 2 (DNA control), lane 3 (DNA+GSH), lane 4 (DNA+GSH+L), lane 5 (DNA+GSH+2), lane

ACCEPTED MANUSCRIPT

6 (DNA+GSH+1) and lane 7 (DNA+GSH+3). Figure B is as same as Figure A, except that GSH was replaced by H_2O_2. Percentage of the nicked circular form was calculated using Image Quant software and indicated above.

In order to get information about the active chemical species which is responsible for the DNA structure, we studied the generation of three activated intermediates, i.e. hydroxyl radical, singlet oxygen and peroxide radical. Figure 10 shows the influence of the radical scavengers on the DNA cleavage of the complexes. Both sodium azide and histidine reduce the DNA cleavage activity by arresting the singlet oxygen or singlet oxygen-like radical species. The DNA cleavage activity is not reduced in presence of DMSO and glycerol (hydroxyl ion scavengers). So, it can be concluded that the complexes follow the oxidative cleavage mechanism with the generation of singlet oxygen species. The complexes with a sulfur atom in their backbone have been shown to react with molecular O_2 or H_2O_2 to produce variety of reactive oxygen species (ROS) [56, 57]. In this mechanism, the reducing agent glutathione initiates the reaction for the generation of the ROS.

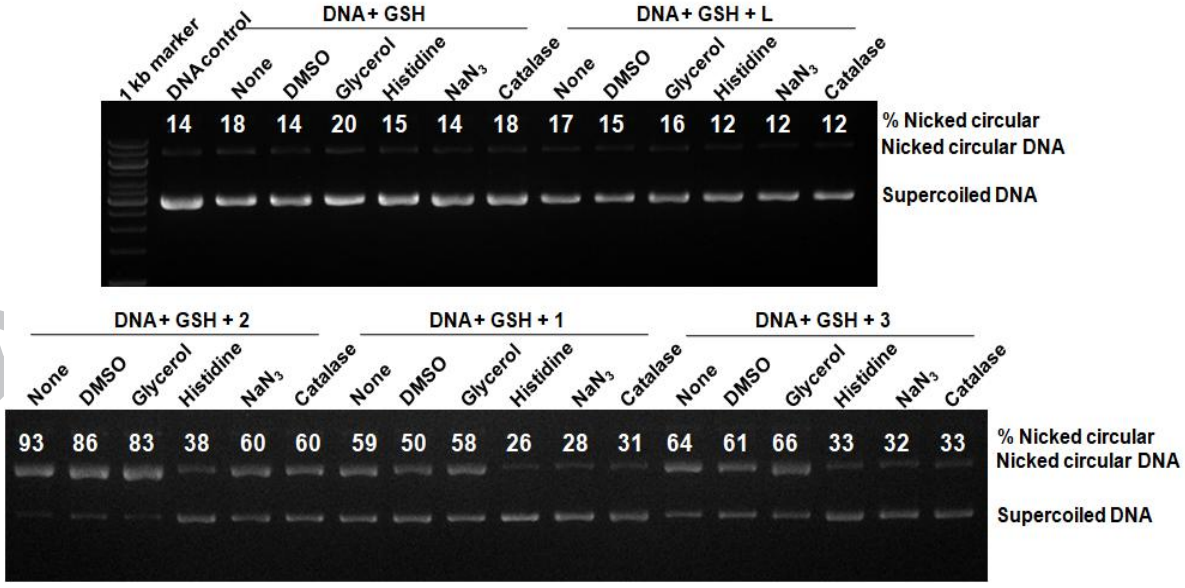

ACCEPTED MANUSCRIPT

Fig 10. Mechanistic studies of the DNA cleavage activity by the copper compounds. Different copper compounds (10 μM) were incubated with 400 ng of pEGFP-C3 DNA for 2 h at 37 °C in a reducing environment consisting of 1 mM of reduced glutathione either alone or in the presence of different ROS inhibitors (DMSO–0.4 M, Glycerol –0.4 M, Histidine –0.1 M, NaN_3–0.1 M and Catalase –10 μg/ml). Plasmids were run on 0.8% agarose gel. The percentage of the nicked circular form was calculated using Image Quant software and indicated above.

Conclusion

An unusual acetonitrile insertion into the exocyclic NH_2 group of 4-(pyridin-2-yl)thiazol-2-amine occurs in the presence of $CuCl_2$ with concomitant formation of stable amidine complexes. The same transformation in the presence of $Cu(ClO_4)_2$ commensurate in the presence of pyrazine, leading to the formation of a pyrazine bridged dinuclear copper(II) complex. All the complexes have been structurally characterized. The amidine complexes (**1** and **3**) show a higher cytotoxicity effect than the free ligand (L) and the non-amidine complex (**2**). The amidine complexes **1** and **3** are identified as potent antiproliferative agents against U937 human monocytic cells with IC_{50} values of 3.7 ± 0.28 and 0.45 ± 0.85 μM, respectively. A DNA binding experiment with CT-DNA reveals the capacity for the formation of Cu(II)complex-CT-DNA species in the order **2** > **1** > **3**. The same order of activity of the reported complexes is also observed with respect to chemical nuclease activity. On the basis of the results, it is evidenced that pyridine thiazole based copper(II)−amidine complexes may be strong candidates for further evaluation as chemotherapeutic agents. This study also provides scope to explore the cytotoxic properties of metal-nucleobase complexes.

Acknowledgements

ACCEPTED MANUSCRIPT

We gratefully acknowledge the Council for Scientific and Industrial Research (CSIR), Government of India for the project grant (No.1(2858)/16/EMR-II). Panskura Banamali College acknowledges the grants that were received from the Department of Science and Technology (DST), Govt. of India through the FIST program (SR/FIST/college-295 dt.18.11.2015). We are also thankful to Dr. Debabrata Maity, Department of Chemistry, Indian Institute of Technology, Bombay, India and Dr. Santanu Pattanayak of National Chemical Laboratory, Pune, India for EPR spectroscopy.

Appendix A. Supplementary data

CCDC 1532570, 1532571 and 1532572 contain the supplementary crystallographic data for complexes **1**, **2** and **3**, respectively. These data can be obtained free of charge via http://www.ccdc.cam.ac.uk/conts/retrieving.html, or from the Cambridge Crystallographic Data Centre, 12 Union Road, Cambridge CB2 1EZ, UK; fax: (+44) 1223-336-033; or e-mail: deposit@ccdc.cam.ac.uk.

Conflicts of interest

There is no conflict of interest to declare.

References

[1] L. M.T. Frijaa, A.J.L. Pombeiro, M. N. Kopylovich, Coord Chem. Rev. 308 (2016) 32.

[2] S. Tadesse, G. Zhu, L.B. Mekonnen, J.L. Lenjisa, M.F. Yu, M.P. Brown, S. Wang, Future Med. Chem. 14 (2017) 1495.

[3] S.Tadesse, M.Yu, L.B. Mekonnen, F. Lam, S. Islam, K. Tomusange, M.H. Rahaman, B. Noll, S. K.C. Basnet, T. Teo, H. Albrecht, R. Milne, S. Wang, J. Med. Chem. 60 (2017) 1892.

[4] N. Misra, H. Y. Xiao, K. S. Kim, S. Lu, W. C. Han, S. A. Barbosa, J. T. Hunt, D. B. Rawlins, W. Shan, S. Z. Ahmed, L. Qian, B. C. Chen, R. Zhao, M. S. Bednarz, K. A. Kellar, J. G. Mulheron, R. Batorsky, U. Roongta, A. Kamath, P. Marathe, S. A. Ranadive, J. S. Sack, J. S. Tokarski, N. P. Pavletich, F. Y. Lee, K. R. Webster, S. D. Kimball, J. Med. Chem. 47 (2004) 1719.

ACCEPTED MANUSCRIPT

[5] Y. Lu, C-M. Li, Z. Wang, J. Chen, M. L. Mohler, Wei. Li, J. T. Dalton, D. D. Miller, J. Med. Chem. 54 (2011) 4678.

[6] M. Li, Y. Sim, S. W. Ham, Bull. Korean Chem. Soc. 31 (2010) 1463.

[7] S. Bondock, W. Khalifa, A. A. Fadda, Eur. J. Med. Chem. 42 (2007) 948.

[8] S. J. Kashyap, V. K. Garg, P. K. Sharma, N. Kumar; R. Dudhe, J. K. Gupta, Med. Chem. Res. 21 (2012) 2123.

[9] L. Labanauskas, V. Kalcas, E. Udrenaite, P. Gaidelis, A. Brukstus, V. Dauksas, Pharmazie 56 (2001) 617.

[10] K. D. Hargrave, F. K. Hess, J.T. Oliver, J. Med. Chem. 26 (1983) 1158.

[11] K. Tsuji, H. Ishikawa, Med. Chem. Lett. 4 (1994) 1601.

[12] R. M. Borzilleri, R. S. Bhide, J. C. Barrish, C. J. D'Arienzo, G. M. Derbin, J. Fargnoli, J. T. Hunt, R. Sr. Jeyaseelan, A. Kamath, D. W. Kukral, P. Marathe, S. Mortillo, L. Qian, J. S. Tokarski, B. S. Wautlet, X. Zheng, L. J. Lombardo, J. Med. Chem., 49 (2006) 3766.

[13] J. Chen, Z. Wang, C. M. Li, Y. Lu, P. K. Vaddady, B. Meibohm, J. T. Dalton, D. D. Miller, W Li, J. Med. Chem. 53 (2010) 7414.

[14] J. Chen, S. Ahn, J. Wang, Y. Lu, J. T. Dalton, D. D. Miller, W. Li, J. Med. Chem. 55 (2012) 7285.

[15] N. Zhang, M. Tomizawa, J. E. Casida, J. Med. Chem. 45 (2002) 2832.

[16] M. Tomizawa, S. Kagabu, I. Ohno, K. A. Durkin, J. E. Casida, J. Med. Chem. 51 (2008) 4213.

[17] H. Elshaflu, S. Bjelogrlic, C. D. Muller, R.T. Todorovic, M. Rodic, M. Marinkovic, N. R. Filipovic, J. Coord. Chem. 69 (2016) 3354.

[18] L. J. Lombardo, F. Y. Lee, P. Chen, D. Norris, J. C. Barrish, K. Behnia, S. Castaneda, A. M. Cornelius, J. Das, A. M. Doweyko, C. Fairchild, J.T. Hunt, I. Inigo, K. Johnston, A. Kamath, D. Kan, H. Klei, P. Marathe, S. Pang, R. Peterson, S. Pitt, G. L. Schieven, R. J. Schmidt, J. Tokarski, M-Li. Wen, J. Wityak, J. Med. Chem. 47 (2004) 6658.

[19] J. D. Crane, A. McLaughlin, Acta Crystallogr., Sect. E. 60 (2004) 0129–0130.

[20] M. J. Frisch, G. W. Trucks, H. B. Schlegel, P. M. W. Gill, B. G. Johnson, M. A. Robb, J. R. Cheeseman, T. Keith, G. A. Petersson, J. A. Montgomery, K. Raghavachari, M. A. Al-Laham, V. G. Zakrzewski, J. V. Ortiz, J. B. Foresman, J. Cioslowski, B. B. Stefanov, A. Nanayakkara, M. Challacombe, C. Y. Peng, P. Y. Ayala, W. Chen, M. W. Wong, J. L. Andres, E. S.

ACCEPTED MANUSCRIPT

Replogle, R. Gomperts, R. L. Martin, D. J. Fox, J. S. Binkley, D. J. Defrees, J. Baker, J. P. Stewart, M. H-Gordon, C. Gonzalez, J. A. Pople, 1995, Gaussian 94, Revision D.1. Gaussian, Inc., Pittsburgh PA.

[21] G. M. Sheldrick, SADABS, University of Göttingen, Germany, 1996.

[22] G. M. Sheldrick, SHELXL-97, Crystal Structure Refinement Program, University of Göttingen, 1997.

[23] T. Mossman, J. Immunol. Methods., (1983) 6555.

[24] K. T. Goswami, B. V. S. Chakravarthi, R. K. Mithun, A. A. Karande, A. R Chakravarty, Inorg. Chem. 50 (2011) 8452.

[25] M. A. O'Neill, J. K. Barton, Top. Curr. Chem. 236 (2004) 67.

[26] J. A. Cowan, Curr. Opin. Chem. Biol. 5 (2001) 634.

[27] D. S. Sigman, R. Landgraf, D. M. Perrin, L. Pearson, Met. Ions Biol. Syst. 33 (1996) 485.

[28] T. Huxel, S. Leone, Y. Lan, S. Demeshko, J. Klingele, Eur. J. Inorg. Chem. 2014 (2014) 3114.

[29] P. Vadivelu, C. H. Suresh, Dalton Trans. 44 (2015) 16847.

[30] G. E. Dobereiner, J. Wu, M. G. Manas, N. D. Schley, M. K. Takase, R. H. Crabtree, N. Hazari, F. Maseras, A. Nova, Inorg. Chem. 51 (2012) 9683.

[31] S. Park, A. L. Rheingold, D. M. Roundhill, Organometallics. 10 (1991) 615.

[32] T. J. Schmeier, A. Nova, N. Hazari, F. Maseras, Chem. Eur. J. 18 (2012) 6915.

[33] B. Longato, D. Montagner, G. Bandoli, E. Zanggrando, Inorg. Chem. 45 (2006) 1805.

[34] A. T. Baker, H. A. Goodwin, A. R. David, Inorg. Chem. 26 (1987) 3513.

[35] C. Pearson, L. A. Bcauchamp, Inorg. Chem. 37 (1998) 1242.

[36] B. Longato, L. Pasquato, A. Mcci, L. Schenetti, Eur. J. Inorg. Chem. 203 (2003) 128.

[37] Reisner, V. B. Arion, A. Rufinska, I. Chiorescu, W.F. Schmid, B. K. Keppler, Dalton Trans. 14 (2005) 2355.

[38] M. Fritz, W.T. Pennington, H.G. Robinson, J. Coord. Chem. 24 (1991) 93.

[39] C. M. Frech, O. Blacque, H. W. Schmalle, H. Berke, Chem. Eur. J. 12 (2006) 5199.

[40] R. M. Ceder,G. Muller, M. Ordinas, J. I. Ordinas, Dalton Trans. (2007) 83.

[41] Y. Zhao, N. E. Schultz, D. G. Truhlar, J Chem. Theory Comput. 2 (2006) 364.

[42] Y. Zhao, D. G. Truhlar, Acc. Chem. Res. 41(2008) 157.

[43] A. Panja, Dalton Trans. 43 (2014) 7760.

ACCEPTED MANUSCRIPT

[44] B. Sarkar, S. Konar, C. J. Gomez-García, A. Ghosh, Inorg. Chem. 47 (2008) 11611.

[45] Y. Hu, C. Y. Li, X. M. Wang, Y. H. Yang, H.L. Zhu, Chem. Rev. 114 (2014) 5572.

[46] A. W. Addison, T. N. Rao, Dalton Trans. (1984) 1349.

[47] A. W. Addison, M. Palaniandavar, W. L. Driessen, F. Paap, J. Reedijk, Inorg. Chim. Acta. 142 (1988) 95.

[48] J. L. Garcıa-Gimenez, G. Alzuet, M. Gonzalez-Alvarez, A. C. Eiras, M, Liu-Gonzalez, J. Borras, Inorg. Chem. 46 (2007) 7178.

[49] G. Beobide, O. Castillo, U. García-Couceiro, J. P. Garcia-Teran, A. Luque, M. Martínez-Ripoll, P. Roman, Eur. J. Inorg. Chem. 2005 (2005) 2586.

[50] J. Borras, G. Alzuet, M. Gonzalez-Alvarez, J. L. Garcia- Gimenez, B. Macias, M. Liu-Gonzalez, Eur. J. Inorg. Chem. 2007 (2007) 822.

[51] A. Kamal, S. Ponnampalli, M. V. P. S. Vishnuvardhan, M. P. N. Rao, Kishore Mullagiri, V. L. Nayaka, B. Chandrakantb, Med. Chem. Commun. 5 (2014) 1644.

[52] K. Zheng, F. Liu, X. M. Xu, Y.T. Li, Z. Y. Wua, C. W. Yan, New J. Chem. 38 (2014) 2964.

[53] S. Zheng, Q. Zhong, Y. Xi, M. Mottamal, Q. Zhang, R. L. Schroeder, J. Sridhar, L. He, H. Mc. Ferrin, G. Wang, J. Med. Chem. 57 (2014) 6653.

[54] Y. Huang, Q.S. Lu, J. Zhang, Z.W. Zhang, Y. Hang, S.Y. Chen, K. Li, X.Y. Tan, H. H. Linb, X. Q. Yua, Bioorg. Med. Chem. 16 (2008) 1103.

[55] A. A. Arbuse, M. Font, M. A. Martínez, M. J. P. Fontrodona, V. Moreno, X. Sala, A. Llobet, Inorg. Chem. 48 (2009) 11098.

[56] J. C. Garcia-Ramos, A. G.t Gutierrez, A. Vazquez-Aguirre, Y. Toledano-Magana, A. L. Alonso-Saenz, V. Gomez-Vidales, M. Flores-Alamo, C.Mejia, L. Ruiz-Azuara, Biometals 30 (2017) 43.

[57] L. F. Hernandez-Ayala, M. Flores-Alamo, S. Escalante-Tovar, R. Galindo-Murillo, J. C. García-Ramose, J. Garcia-Valdes, V. Gomez-Vidales, K. Resendiz-Acevedo, Y. Toledano-Magana, Lena Ruiz-Azuara, Inorg. Chim. Acta 470 (2018) 187.

ACCEPTED MANUSCRIPT

Copper assisted acetonitrile insertion into 2-amino-4-(2-pyridyl)thiazole (**HL**) conferred the nitrile to amidine transformation; an unusual formation of mono and dinuclear copper(II)-amidine complexes with the composition $[Cu\{\mathbf{L}C(Me)=NH)\}Cl_2]$ (**1**) and $[(ClO_4)\{\mathbf{L}C(Me)=NH)\}Cu(\mu\text{-pyrazine})Cu\{\mathbf{L}C(Me)=HN\}(ClO_4)](ClO_4)_2$ (**3**). The same reaction with copper(II) perchlorate and **HL** yielded the complex $[Cu(\mathbf{HL})_2](ClO_4)_2$ (**2**) where no acetonitrile addition was observed. The complexes show significant programmed cell death in human monocytic cells (U937). The chemical nuclease activities of complexes **1**, **2** and **3** respectively show 65, 99 and 80 % relaxation of supercoiled DNA at 10 μM in the presence of glutathione (GSH, 1 mM) following an oxidative cleavage mechanism.